The Influence of Elbow Flexion and Arm External Rotation on Peak Elbow Valgus Torque and Ball Velocity in Baseball Pitching

by

L.W. Vliegen, BSc

in partial fulfilment of the requirements for the degree of

Master of Science
in Mechanical Engineering

at the Delft University of Technology,
to be defended publicly on Friday January 26, 2018 at 10:00 AM.

Student number:	4330862	
Master track:	Biomechanical Design	
Specialization:	Sports Engineering	
Thesis committee:	Prof. dr. H. E. J. Veeger	TU Delft, supervisor
	Dr. D. J. J. Bregman	TU Delft
	Dr. ir. A. J. Jansen	TU Delft

The influence of elbow flexion and arm external rotation on peak elbow valgus torque and ball velocity in baseball pitching

Master thesis Liset Vliegen, TU Delft, Faculty of 3ME, Biomechanical Design

Abstract

Introduction Elbow injury, especially Ulnar Collateral Ligament (UCL) tear, is very common in baseball pitching. This is often attributed to high valgus torques repetitively stressing the ligament. The goal of this study was to research the effect of Elbow Flexion (EF) and arm External Rotation (ER) angle on Peak Valgus Torque (PVT) as well as ball velocity, using a three-folded approach.

Methods Motion data of 12 Dutch A and AAA team pitchers were collected (29 pitches in total). Firstly, the relationships between the variables and outcomes were statistically evaluated with Generalized Estimating Equations (GEE). Secondly, simplified movements and EF and ER variations were input to a two-segment model, which was based on the hypothesis that valgus torque is generated by inertial effects from external rotation deceleration and forearm forward acceleration. Lastly, for one pitch per player, ER and EF angles were varied in simulations.

Results Statistical significance was only observed for higher EF as a predictor of increased PVT and higher ER as a predictor of decreased ball velocity. In the two-segment model, PVT increased for higher EF and decreased for higher ER. The simulations showed different effects between pitchers, however, most trends were similar to those of the two-segment model. Ball velocity was maintained or increased with higher EF, while the influence of ER on ball velocity differed between players.

Conclusion The two-segment model led to a more in-depth insight in the many factors influencing PVT in pitching. The results of this study suggest that higher ER and lower EF could lead to lower PVT, without necessarily giving in on performance. However, the results showed differences between pitchers. As previous studies reported opposite trends regarding ER, we believe that this discussion should be re-opened. Our findings suggest that some pitchers are more prone to elbow injury than others and that pitchers might be able to lower injury-risk by adapting their pitching technique.

1 Introduction

1.1 Background and research goal

Baseball pitching is a highly dynamic movement that shows high injury rates. In 1989-1999, 45% of the injured Major League Baseball (MLB) players were pitchers (Conte et al., 2001). In this study, 22% of the playing loss days were because of elbow injury. Another study reported that 26% of the 298 youth pitchers experienced elbow pain, of which 68% were on the medial side (Lyman et al., 2001).

A common elbow injury on the medial side is ulnar collateral ligament (UCL) tear. A study among 2500 professional baseball pitchers found that 16% had a history of UCL reconstruction (Conte et al., 2015). The incidence of UCL reconstructions is growing, especially in teenagers (Erickson et al., 2015). Even in asymptomatic players, abnormalities in the UCL have been observed (Kooima et al., 2004). For safe and injury-free pitching, research into elbow injury prevention is therefore very important.

Elbow injury in pitching is often attributed to high valgus torques. Valgus torque, which is commonly encountered in pitching (Hariri and Safran, 2010), is an external torque that the forearm exerts on the elbow joint, attempting to rotate the forearm to the lateral side with respect to the upper arm. This movement is normally restrained by counteracting internal varus torques, imparted on the forearm by elbow joint structures, most notably the UCL. The external valgus torque imparts a tensile force to the medial and a compressive force to the lateral elbow structures. This can result not only in injury to the medially located UCL, but also to the medial muscles and ulnar nerve and in damage of the radiocapitellar joint on the lateral side (Safran et al., 2005; Cain et al., 2003). In fact, higher peak valgus torques were found in pitchers suffering from elbow injury and pitchers with abnormal UCL appearance than in asymptomatic pitchers (Anz et al., 2010; Hurd et al., 2011). Understanding about how Peak Valgus Torque (PVT)

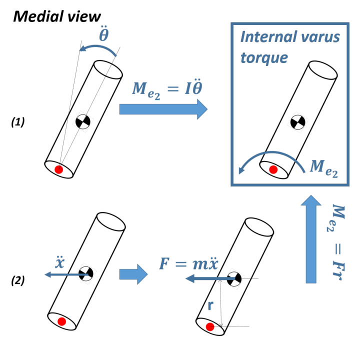

Figure 1: Two mechanisms can theoretically generate internal varus torque in pitching: (1) rotational inertia and (2) translational inertia. The external valgus torque that the forearm exerts on the joint structures is equal to the internal varus torque.

can be lowered, while keeping up high performance levels, may help pitchers to prevent elbow injury.

Theoretically valgus torques in pitching can be generated by two mechanisms (Figure 1): (1) rotational inertia: a resistance to angular acceleration/deceleration, leading to a torque; and (2) translational inertia: a resistance to linear acceleration/deceleration results in an inertial force on the center of mass (CoM), generating a torque around the elbow joint. The magnitude of the valgus torque depends on the posture of the body as well as the accelerations and thus it is affected by adjusting pitching technique. This study focuses on the effect of humerothoracic External Rotation (ER) and Elbow Flexion (EF) angle, as they highly influence the orientation of the forearm and hand.

Some studies have related these parameters to valgus torque. Aguinaldo and Chambers (2009) and Sabick et al. (2004) reported that higher Maximum External Rotation (MER) correlated with higher PVT. Lower EF (a more extended elbow) was reported to correlate with higher PVT (Aguinaldo and Chambers, 2009; Werner et al., 2002) and with higher risk at medial elbow pain (Huang et al., 2010). However, these correlations do not give any in-depth understanding on how high valgus torques develop as a result of the pitching technique. In addition, the correlations do not necessarily indicate causality and the effect can not be extrapolated outside of the measured range of the data. These problems can be overcome by simulations, controlling the specific variable of interest.

Moreover, higher MER and lower EF were also reported to correlate with ball velocity (Fortenbaugh et al., 2009; Huang et al., 2010), while the aforementioned studies did not correct for this, nor did they report correlations with ball velocity. Research on the influence of technique parameters on both PVT and ball velocity is scarce. Therefore, the goal of this study was to thoroughly analyze how humerothoracic external rotation and elbow flexion influence peak valgus torque and ball velocity in baseball pitching.

First, a theoretical problem analysis is carried out to form a hypothesis. Subsequently these hypotheses are tested using pitching data from previous studies, according to a three-folded approach:

1. Statistical analysis: do we find a significant relationship between the variables and Peak Valgus Torque and ball velocity in the data?
2. Two-segment model: simplifying the pitching movement to understand the mechanisms contributing to high valgus loads.
3. Simulations: tweaking the joint angles for all subjects to research its influence on PVT and ball velocity within the complex movement.

1.2 Analysis and hypothesis

Joint torques and forces can be defined in the proximal or distal Segment Coordinate System (SCS) or projected onto Euler rotation axes. The upper arm (proximal) SCS does not rotate with elbow flexion, while we are interested in an expression that accounts for stress on medial and lateral elbow structures in all flexion angles. The forearm (distal) SCS is irrelevant for the elbow as it rotates with pronation/supination. Therefore, we define valgus/varus torque as the projection of the net torque vector on the floating X-axis perpendicular to the plane spanned by the humerus Z_h and the ulnar Y_u axis from the respective segment coordinate systems (SCS) (Figure 2).

NB:The definition of the Z_h axis in the humeral SCS is an estimation of the flexion-extension axis that cannot be assured to be equal to the joint rotation axis. This may result in projections of flexion/extension rotation/torque on the varus/valgus or pro-/supination axis.

In pitching research, the pitching movement is typically divided into six phases, defined by five key events (Figure 3). The peak valgus torque (PVT) was reported to occur in the late cocking phase of the movement, just before Maximal External Rotation (MER) (Fleisig et al., 1995; Sabick et al., 2004; Werner et al., 1993). In this phase, we hy-

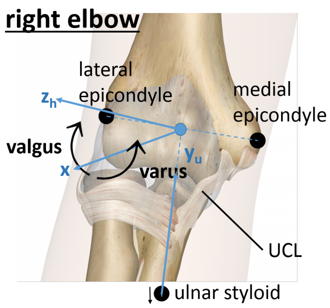

Figure 2: Floating $x-$axis for varus/valgus torque projection: perpendicular to the humerus z_h and the ulnar y_u axes.

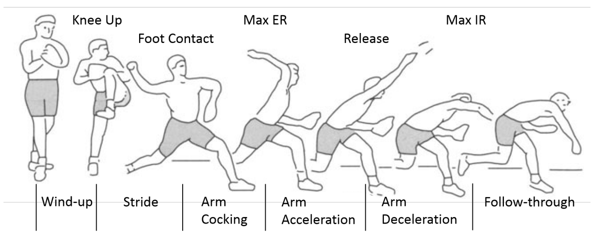

Figure 3: Six phases and five key events of the pitching movement (adapted from Fleisig et al. (1996)).

pothesize that valgus torque is mainly generated by the following rotational inertia (1) and translational inertia (2) mechanisms: (1) Before MER, the external rotation is slowed down by an internal rotation torque that shoulder joint structures exert on the upper arm. This gives the forearm an angular deceleration, which results in an inertial valgus torque. (2) A forward acceleration of the forearm (from full body forward acceleration, thorax axial rotation and shoulder horizontal abduction) results in an inertial force on the center of mass (CoM), generating a valgus torque.

A higher arm External Rotation (ER) angle results in a shorter moment arm with respect to (2), while it does not influence (1) provided that the angular accelerations are the same (Figure 4). Therefore, we hypothesize that higher ER leads to lower PVT.

When the Elbow Flexion (EF) angle is close to 90°, the shoulder internal/external rotation axis (s_2) and the elbow varus/valgus axis (e_2) align, leading to a maximum forearm valgus angular deceleration induced by the internal rotation torque (1). Higher and lower EF angles change the direction of the varus/valgus axis, lowering the angular deceleration and thus lowering valgus torque (Figure 5). EF angle does not influence the moment arm of the inertial force with respect to the varus/valgus axis (2). However, forearm CoM acceleration (2) due to shoulder horizontal abduction and thorax axial rotation increases with elbow flexion as the distance to the rotation axes increases.

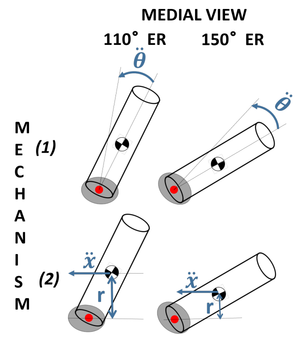

Figure 4: The hypothesized effects of External Rotation (ER) on the two mechanisms that generate valgus torque.

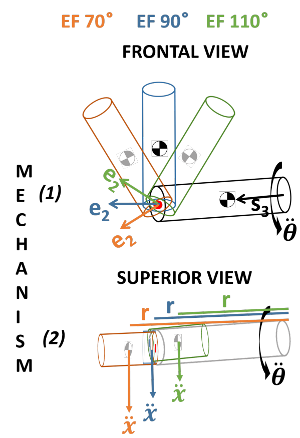

Figure 5: The hypothesized effects of Elbow Flexion (EF) on the two mechanisms that generate valgus torque.

2 Methods

2.1 Data collection

The subjects of this study were eight right-handed pitchers from the Dutch AAA team (age: 16.3±0.7 years, weight: 77.9±8.9 kg, length: 184.4±6.5 cm) and four right-handed pitchers from the Dutch A team (age: 28.3 ± 5.3 years, weight: 98.3 ± 4.6 kg, length: 193.3 ± 3.8 cm). The research project was approved by the Faculty of Human Movement Sciences' local ethical committee and informed consent was signed by the participants and/or their legal tutor.

The pitchers were equipped with a full body marker set. In this study, the thorax and right upper limb markers were used for kinematics and dynamics and the knee and ankle markers for phase estimation. After a warm-up, they performed five fastball pitches from a pitching mound. The marker trajectories were recorded by a 10-camera (T40S, 100Hz) VICON system. The data were interpolated to correct for occlusions and filtered with a 4th order Butterworth 12.5 Hz low-pass filter. Based on the quality of the data, 29 pitches (1-3 pitches per player) could be used for this study.

2.2 Rigid body model

A rigid body model of the thorax and right upper limb was used, based on the mean measured local marker positions within each segment. The Segment Coordinate Systems (SCS) and Joint Coordinate Systems (JCS) were based on ISB recommendations (Wu et al., 2002, 2005) (Appendix A). The ulnohumeral JCS was used for the elbow and the humerothoracic JCS for the shoulder. Regression equations from Dumas et al. (2007) were used to determine the gleno-humeral joint position, the positions of segment Centers of Mass (CoM) and the segment masses and inertia matrices.

The right shoulder, elbow and wrist were modeled as spherical joints with 3 rotational degrees of freedom. The glenohumeral joint additionally had 3 degrees of freedom to model the motion of the scapular girdle in a simplified way. The ball was modelled as a sphere with a 36.8mm radius and a weight of 145g, according MLB rules. The CoM was assumed to be in the same position as the hand CoM. Ball release was modelled as a 100% to 0% decreasing ball mass during the second half of the acceleration phase, approximated as 20 ms.

2.3 Kinematics and inverse dynamics

For kinematics and inverse dynamics, the wrench and quaternion method as described by Dumas et al. (2004) was used. Quaternions are a representation of the segment attitude (alternative for the rotation matrix R) that uses a vector and the rotation around that vector. Wrench is a mechanical notation that represents forces and moments together in a 6D vector. These were all expressed in the inertial coordinate system (ICS), so that no transformations between SCSs were necessary. This inverse dynamics method was used to determine the net moments at the wrist, elbow and shoulder in the ICS, using a distal to proximal sequence. No external forces (except for gravity) act on the distal segment. The net moments at the joints are calculated as the torque exerted by the proximal segment on the proximal end of the distal segment.

Humerothoracic and elbow joint angles and thorax angles relative to the global coordinate system are calculated according to the Euler angles defined by Wu et al. (2005) (Y-X-Y, Z-X-Y and Z-X-Y order respectively, Figure 6). Varus/valgus torque M_{e_2} is defined as the projection of the net elbow torque vector on the elbow floating rotation axis ($\mathbf{e_2}$) and it is calculated for every frame:

$$M_{e_2} = \mathbf{M}^{\mathbf{ICS}}_{\mathbf{elbow}} \cdot \mathbf{e_2} \tag{1}$$

NB: a positive M_{e_2} elbow joint moment represents an internal varus moment exerted on the forearm, or - as it is equal and opposite - an external valgus moment loading the joint structures. Similarly, elbow flexion torque M_{e_1} is calculated as

$$M_{e_1} = \mathbf{M}^{\mathbf{ICS}}_{\mathbf{elbow}} \cdot \mathbf{e_1} \tag{2}$$

Similarly, this represents an internal elbow flexion moment that is exerted on the forearm by the joint structures.

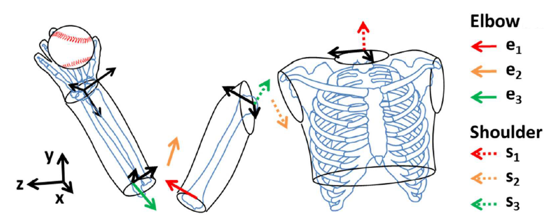

Figure 6: Joint rotation axes for Euler angles and joint torque projections.

2.4 Data processing

The pitch was subdivided in the six phases as customary in pitching research (Figure 3). The end of the wind-up phase (WU) was estimated using the highest point of the knee joint center of the stride leg. Foot contact (FC) was defined using the forward velocity of the stride leg ankle joint center (threshold 0.3 m/s). Maximum external and internal rotation (MER and MIR) are the times of minimum and maximum s_3 Euler angle before and after ball release respectively. An estimation of ball velocity and the time of ball release (BR) was made using the maximum forward linear velocity of the middle finger distal interphalangeal marker (RHID3).

The mean and standard deviation between pitchers of the Elbow Flexion and External Rotation angle at the times of PVT and MER were calculated. Additionally, the mean and standard deviation of the forearm CoM forward acceleration was calculated.

2.5 Statistical analysis

The linear relationship between the predictor (EF, ER) and the dependent variable (PVT, ball velocity) was estimated using Generalized Estimating Equations (GEE). GEE is a modeling of the mean (just as an ordinary regression analysis) that can account for multiple observations per subject: observations are not assumed to be independent as a correlation structure between the observations of the same subject are taken into account (Moen et al., 2016). The relationship is expressed in the form of $y = a + bx$ and significance of the estimated factor b is tested ($P < 0.05$).

2.6 Two-segment model

A simple two-segment model was made in MATLAB, consisting of an upper arm and a forearm-hand segment. Segment mass and length were defined as the averages of the subject data and the inertia and CoM properties were derived with regression equations from Dumas et al. (2007) (Table 1). Only the cocking phase (Figure 3) was modelled. Thorax axial rotation was only taken into account as a reference for shoulder angles, to calculate upper arm position.

Reference posture In all cases, the displacements and angles other than the defined movements and variables (described below) were kept constant as in the following reference posture: the shoulder joint stays at (0,0,0); the shoulder has 0° horizontal abduction, 80° abduction and 90° external rotation; the elbow has 90° flexion, 0° abduction and 100° of pronation. This reference posture was based on the average values in the cocking phase of the subject data (Appendix C).

Movements The model was subjected to three simple movements: (1) external rotation, (2) horizontal abduction and (3) acceleration. For (1) and (2), the input was the average shoulder joint angle time series of the total 29 pitches, relative to the global reference frame (assuming an upright, forward facing stationary thorax). For (3), the input was the average shoulder x- and z- displacement and the shoulder angles were defined relative to an axially rotating thorax (average time series). In the last simulation (4), the three movements were combined.

Variables (Overview: Table 2) PVT dependency on Elbow Flexion was tested in two ways: constant and dynamic. Constant: EF was defined as a constant value, varying between 60° and 110° (5° steps). Dynamic: EF was the mean curve $\pm$ 5-25° in 5° steps. In this case, the elbow started extending before MER. External Rotation was varied using the mean curve $\pm$ 5-25° in 5° steps. The combined effect of EF and ER was lastly tested using all possible combinations of the above EF and ER values, for movement (4).

With the described input of angles and shoulder coordinates, the transformation matrices were calculated (Appendix B) and subsequently used for the inverse dynamics calculations.

2.7 Simulations

For all 12 pitchers, one pitch was chosen for simulations (the first pitch in case of two pitches and the one with intermediate PVT in case of three pitches). For these 12 pitches the EF and ER angles (EF_0 and ER_0) were calculated and then varied (overview: Table 2). The variation (ΔEF and ΔER) was based on the within and between pitcher variation in the data (Appendix E): $\Delta EF = \pm 1 - 5°$ in steps of 1°; and $\Delta ER = \pm 2 - 10°$ in steps of 2°.

The variations for EF were made in two different ways (Figure 7):

(1) Shifted: $EF = EF_0 + \Delta EF$ for all frames. This method keeps angular accelerations the same.

(2) Scaled: at PVT, $EF = EF_0 + \Delta EF$. Leading up to and after PVT, the EF was scaled (Appendix D). The angular accelerations change, but this method showed to correct for ball velocity ($< 1\%$ deviation from the original). As the flexion angular accelerations change, the influence of the scaled EF on peak elbow flexion torque was evaluated.

The variations for External Rotation were made only in the first way (1), because ball velocity correction was not feasible for this simulation.

With these angles, the transformation matrices were recalculated for the upper arm and forearm segment (Appendix B) and used to recalculate the inverse dynamics calculations. Additionally, the local RHID3 position in the hand SCS of the original data was used to estimate the ball velocity of the simulation. To account for ball velocity changes, the ratio PVT/ball velocity (PVT/BV) was calculated (a lower ratio is preferable). Additionally,

segment	mass	length	x_{com}	y_{com}	z_{com}	I_{xx}	I_{yy}	I_{zz}	I_{xy}	I_{yz}	I_{xz}
Upper arm	1.8956	0.3410	0.0091	-0.1542	-0.0063	0.0221	0.0045	0.0236	8.28e-4	9.20e-5	5.75e-4
Forearm-hand	1.9780	0.3593	0.0051	-0.2265	-0.0063	0.0637	0.0041	0.0637	0.0012	-0.0012	3.92e-4

Table 1: Methods: Properties of the segments in SI units. Segment mass (kg), length (m), center of mass (com) position in the SCS (m), inertia in the SCS (kg·m^2).

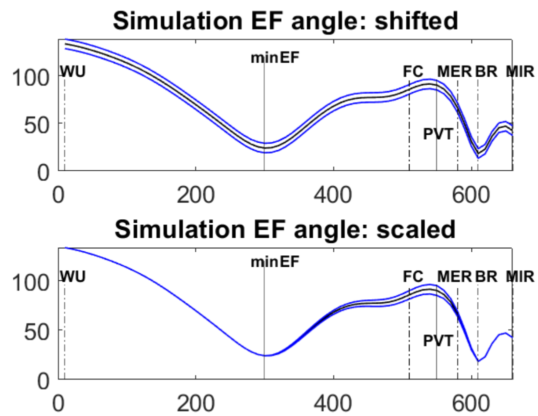

Figure 7: Methods - simulations: two ways of varying the Elbow Flexion (EF) angle (example data of one pitcher). Black: original. Blue: $\pm 5°$ variations.

the % average deviation of the simulation from the original ball velocity is calculated as well as the maximum % deviation. Lastly, the effect of the simulations on the timing of ball release was evaluated.

	Two-segment model	Simulations
EF	constant $60-110°(\Delta 5°)$	shifted $data \pm 5°(\Delta 1°)$
	dynamic $mean \pm 25°(\Delta 5°)$	scaled $@PVT : data \pm 5°(\Delta 1°)$ $@BR : original$
ER	dynamic $mean \pm 25°(\Delta 5°)$	shifted $data \pm 10°(\Delta 2°)$
Combination	constant EF + dynamic ER	
	dynamic EF + dynamic ER	

Table 2: Methods: Overview of the changes made to the data in the two-segment model and the simulations. $mean$ = mean time series over all pitches. $data$ = data of the individual 12 chosen pitches. Δ = the interval between modeled EF and ER angles.

3 Results

The average Peak Valgus Torque (PVT) across all pitches was 69.8 ± 9.8 Nm and occurred on average at two-third ($67.2 \pm 16.0\%$) of the cocking phase, before MER (Figure 8). Ball velocity was 28.6 ± 1.6 m/s. At the instant of PVT, Elbow Flexion (EF) was $85.9 \pm 7.7°$ and External Rotation (ER) was $138.4 \pm 14.0°$. At the instant of MER, EF was $68.3 \pm 9.9°$ and ER was $154.6 \pm 12.0°$. Throughout the cocking phase, the forearm showed a CoM acceleration with its peak at the same instant as PVT (Appendix C).

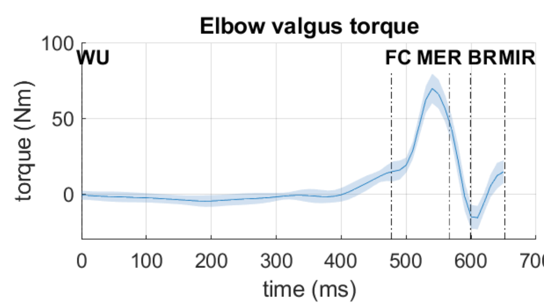

Figure 8: Results: Elbow valgus torque mean $\pm$ SD over all 29 pitches. For reference, the mean timing of the key events is denoted above.

3.1 Statistical analysis

The Generalized Estimating Equations (GEE) analysis (Table 3, Figure 9) showed that Elbow Flexion was a significant ($P < 0.05$) predictor of PVT, but not of ball velocity. External Rotation was not a significant predictor of PVT, but the predicting factor of ER on ball velocity was small though significant.

3.2 Two-segment model

Figures 10 and 11 show the relationship between EF/ER angle and the peak (negative) valgus torque for all movements. Extensive time plots of the described results (including the movement and variable inputs and PVT and forearm CoM acceleration outcomes) are added in Appendix F.

dependent variable	predictor	b	p
PVT	EF	0.515	0.041
	ER	0.111	0.368
Ball velocity	EF	-0.098	0.811
	ER	-0.02	0.000

Table 3: Results - statistical analysis: The outcome of the Generalized Estimating Equations (GEE) - factor b ($y = a + bx$) and its associated significance value p for GEE relating predictors (x) Elbow Flexion (EF) and External Rotation (ER) to dependent variables (y) Peak Valgus Torque (PVT) and ball velocity.

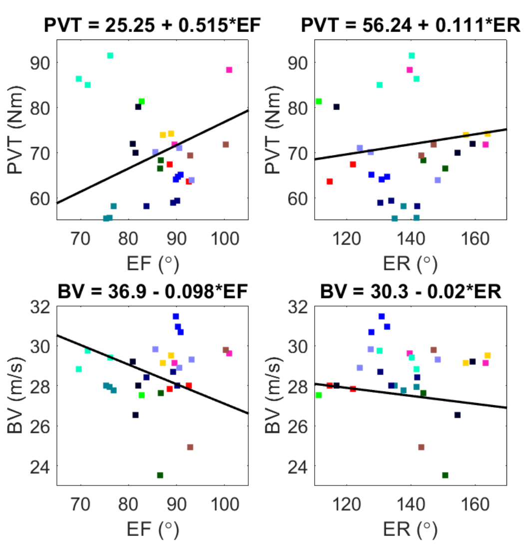

Figure 9: Results - statistical analysis: The estimating equation plotted over the data points (a different colour for every subject). Only the upper left and lower right estimations were significant.

Elbow Flexion *Movement (1) External rotation:* assuming constant EF, a maximum PVT was observed slightly above 90°. For dynamic EF, PVT increased with flexion angle and PVT occurred later for higher EF angle. The movement resulted in forearm/hand CoM accelerations, which were higher for dynamic EF. *(2) Horizontal abduction:* negative valgus torques were observed, which decreased with EF angle in both cases. The movement resulted in CoM decelerations. *(3) Acceleration:* a negative valgus torque was observed, which decreased with EF angle. In case of high dynamic EF angles, this was an increasing small valgus torque. The movement resulted in CoM decelerations. *(4) Combination:* A maximum PVT was observed at 100° for constant EF. For dynamic EF, the PVT was higher and it increased with EF angle. The movement resulted in CoM decelerations close to MER for constant EF and accelerations for dynamic EF, although lower values than in case of (1).

External Rotation In the movements (1), (2) and (3), PVT was at the time of MER. *Movement (1) External rotation:* PVT showed a very small increase with increasing MER. The movement resulted in CoM accelerations which decreased with increasing ER. *(2) Horizontal abduction and (3) acceleration:* PVT increased significantly with increasing MER angle. *(4) Combination:* PVT increased significantly with increasing ER. The trend switching from rounded to straight came from the difference in timing of PVT: earlier for lower MER angles. Movements (2-3) resulted in CoM accelerations for lower ER angles and decelerations for higher ER angles. Movement (4) resulted in CoM decelerations for most ER angles, but accelerations for lower ER.

EF and ER combined When the variations of ER was combined with dynamic EF (extending elbow), PVT decreased with increasing External Rotation, opposite to the case where constant EF was assumed. The other trends were similar to those of the isolated variations (Figure 12).

3.3 Simulations

Elbow Flexion PVT increased with EF for nine pitchers and decreased for three pitchers (Figure 13). Ball velocity increased with EF for all pitchers (average deviation from the original ball speed 5.97%, max deviation 6.55%). PVT/BV ratio showed no obvious trend for four pitchers, but decreased with EF angle for the other eight pitchers. A two-tailed t-test did not reveal any sig-

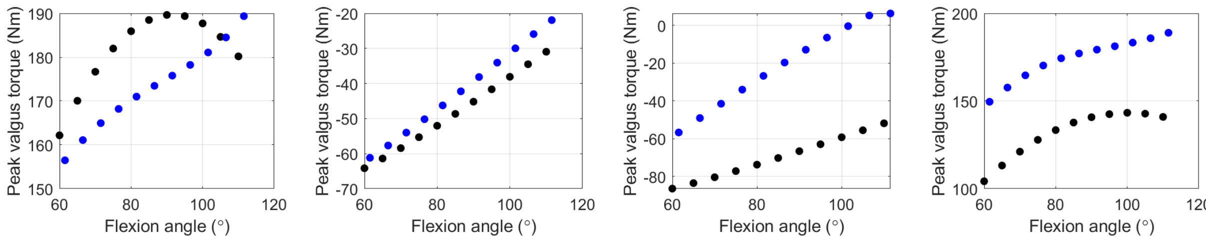

(a) 1. External rotation (b) 2. Horizontal abduction (c) 3. Forward translation (d) 4. Combined

Figure 10: Results - two-segment model: plots of the Elbow Flexion (EF) angle (x-axis) versus the Peak Valgus Torque (PVT) (y-axis) for four movements. Black: contant EF. Blue: dynamic EF (EF value at 2/3 of cocking phase plotted).

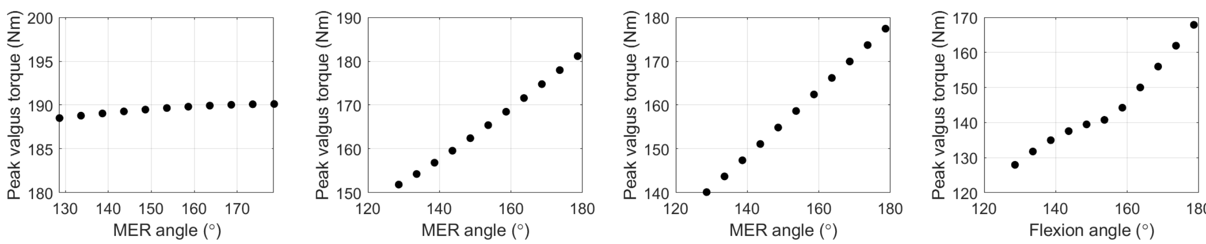

(a) 1. External rotation (b) 2. Horizontal abduction (c) 3. Forward translation (d) 4. Combined

Figure 11: Two-segment model: Plots of the simulated Maximal External Rotation (MER) angle (x-axis) versus the Peak Valgus Torque (PVT) (y-axis) for four movements.

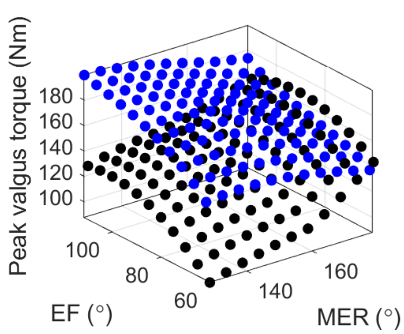

Figure 12: Results - two-segment model: 3D plot of the combined effect of Elbow Flexion (EF) and Maximal External Rotation (MER) angle. Black: constant EF. Blue: dynamic EF (EF value at 2/3 of cocking phase plotted).

nificant differences between the baseline data of the increasing/decreasing PVT groups (team, age, weight, height and range of motion).

The scaled EF simulations showed a ball velocity close to the original pitches (average deviation 0.49%, maximum deviation 0.75%). PVT increased with EF angle for nine pitchers, decreased for one pitcher and showed no obvious trend for two pitchers (Figure 14). PVT/BV ratio increased with EF for three and decreased for three pitchers. For one pitcher, the elbow flexion torque increased due to the simulation method. For the other eleven pitchers, only slight increases or decreases were observed (Appendix D). The timing of ball release was not affected by the simulations.

External Rotation Patterns of ER vs. PVT were very inconsistent between pitchers (Figure 15). The biggest group (six out of twelve pitchers) showed a decreasing PVT for higher ER. For four pitchers, PVT showed a maximum, but at different ER angles. PVT increased with higher ER for two pitchers. Ball velocity showed an optimal ER angle for eight pitchers, although at different values. Two pitchers showed unclear relationships, for one pitcher ball velocity increased and for one it decreased with ER. Ball velocity deviated from the original pitch with a mean of 2.46% and a max of 4.85%. PVT/BV ratio decreased with ER for

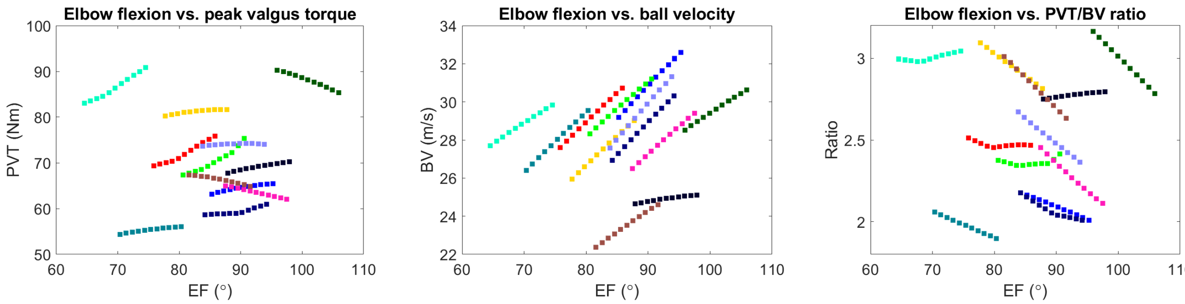

Figure 13: Results - simulations: shifted Elbow Flexion (EF): effect of EF (value at original time of PVT) on Peak Valgus Torque (PVT), ball velocity and PVT/BV ratio. Each color represents simulated values for one pitcher.

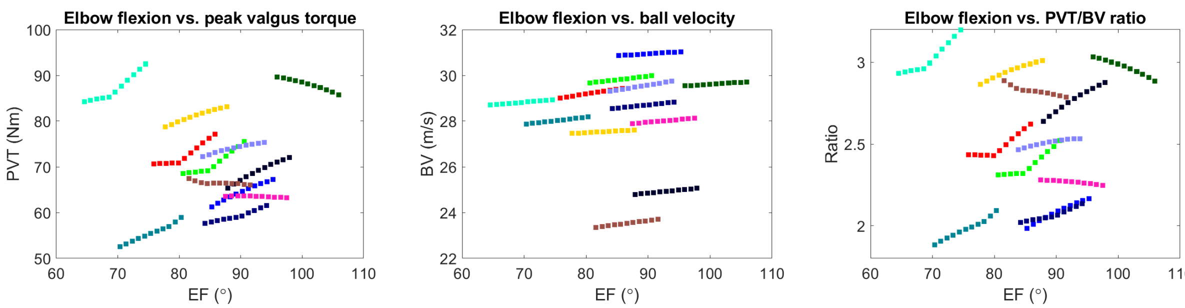

Figure 14: Results - simulations: scaled Elbow Flexion (EF): effect of EF (value at original time of PVT) on Peak Valgus Torque (PVT), ball velocity and PVT/BV ratio. Each color represents simulated values for one pitcher.

six pitchers, showed only small deviations for four pitchers and showed unclear trends for 2 pitchers. Two separate clouds arose: low ER/low ratio and high ER/high ratio. A two-tailed t-test did not reveal any significant differences in baseline data (team, age, weight, height and range of motion) between the two groups. The timing of ball release was not affected for ten pitchers, but for one pitcher it occurred 10 ms earlier (red plots) and for one pitcher 20 ms earlier (black plots) for some ER variations (both higher and lower ER variations).

4 Discussion

4.1 Results

The high incidence of elbow injury, especially to the UCL, has been linked to recurring high valgus torques occurring in the late cocking phase of the pitching movement. This study was carried out in order to investigate how Elbow Flexion (EF) and arm External Rotation (ER) variations affect Peak Valgus Torque (PVT) and whether they also influence ball velocity.

In the data, an average PVT of 69.8 Nm occurred at 67% of the cocking phase. An average ball velocity of 28.6 m/s (64.0 mph) was observed. The statistical analysis (Generalized Estimating Equations, GEE) showed that PVT increased significantly with a greater Elbow Flexion angle, while its effect on ball velocity was not significant. The effect of External Rotation on PVT was not significant, but ball velocity showed a slight but significant decrease for a further externally rotated arm. The two-segment model showed that the influence of EF and ER on PVT was different when the elbow extension at the end of the cocking phase was modeled, compared to the case where the EF angle was assumed constant. Taking the elbow extension into account, PVT increased for a more flexed elbow (higher EF) and a less externally rotated arm (lower ER). The results of the simulations indicated that the effect of EF and ER on PVT differs between pitchers. By keeping the EF angle at ball release the same as in the original data, ball velocity was kept nearly constant ($< 1\%$ change). In this case, PVT increased with greater elbow flexion. A narrow majority of the pitchers showed decreasing PVT for higher External Rotation, while no pattern was found in the effect on ball velocity. The conclusions from the three methods are summarized in Table 4.

The average peak valgus torque of 69.8 Nm calculated from the original data is similar to literature

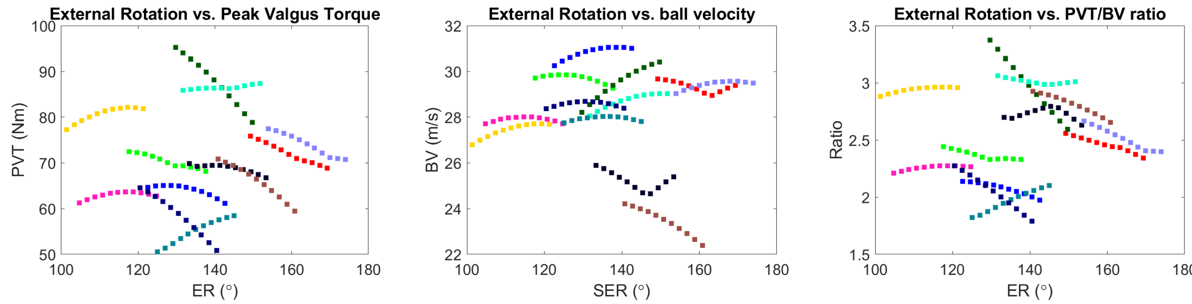

Figure 15: Results - simulations: effect of External Rotation (value at original time of PVT) on Peak Valgus Torque (PVT), ball velocity and PVT/BV ratio. Each color represents simulated values for one pitcher.

		EF	ER
PVT	statistics	+ (sig.)	+
	two-segment	+	−
	simulations	diff/+	diff/−
BV	statistics	−	− (sig.)
	two-segment	n.a.	n.a.
	simulations	+/0	diff

Table 4: Overview of the results from the statistical analysis (GEE), two-segment model and simulations. + indicates a positive relationship, − a negative relationship and 0 no (clear) relationship. sig. = significance in the GEE; diff = different relationships among the subjects in the simulations; n.a. = not applicable (not modeled).

values, which are usually reported around 50-65 Nm for adult pitchers (Aguinaldo and Chambers, 2009; Fleisig et al., 1995; Gasparutto et al., 2016; Matsuo et al., 2006). Previous research agreed with our finding that PVT occurred in the last part of the cocking phase, but the timing in this study was slightly earlier than previously reported: 67% of the cocking phase versus approximately 75% or later (Fleisig et al., 1995; Werner et al., 1993; Sabick et al., 2004; Zheng et al., 2004).

Ball velocity was estimated by the peak forward velocity of the RHID3 marker as 28.6 m/s (64.0 mph) on average. However, baseline data showed an average of 35.8 m/s (80 mph). The discrepancy could result from two issues. First of all, in most cases the ball is not thrown precisely along the forward direction. However, this method was chosen because it leaves out finger movements that might have a high velocity in a different direction than the ball. Second of all, the relatively low frequency of the data acquisition could have cut off high velocity peaks.

Two-segment model: evaluation To analyze how high valgus torques develop, the two-segment model was used. It was based on the hypothesis that valgus torque is generated by inertial effects from external rotation angular deceleration and forearm forward acceleration. Forearm forward acceleration was assumed to be resulting from shoulder displacement, thorax axial rotation and shoulder horizontal abduction.

The modeled movements (2 and 3) that did not include external rotation showed a decelerating forearm CoM close to MER. When external rotation was applied (movements 1 and 4), the forearm CoM accelerated, as it did in the original data. At first glance, this opposes our intuition, as external rotation brings the forearm further backward. However, this external rotation is decelerated, which leads to a net forearm/hand CoM acceleration. Thus, although valgus torque is indeed partly generated by inertial effects from forearm forward acceleration, our problem analysis did not describe the complete mechanism. Apart from thorax rotations, shoulder displacement (from full body accelerations) and horizontal abduction, forearm CoM acceleration is also caused by external rotation deceleration.

Additionally, we modeled the elbow flexion angle in two ways: constant (90°) and dynamic (extending before MER). In the case of constant EF, we found forearm CoM deceleration close to MER, while the results assuming an extending elbow as well as the original data showed accelerations. Indeed, when the arm is externally rotated more than 90°, elbow extension brings the forearm forward. Thus, elbow extension acceleration leads to forearm CoM forward acceleration. The constant elbow flexion angle therefore appeared to be an oversimplification. Consistently, the curve of valgus torque over time resembled the actual data more when elbow extension was modeled. As explained in the problem analysis (Figure 5), the projection of External Rotation deceleration on the valgus axis depends on the EF angle. In the cocking phase, the values of that ER angular deceleration as well as the EF angle change over time. Consequently, the magnitude of the valgus torque at an instant (and thus also the timing of PVT) depends on the interaction between those two.

When elbow extension in the cocking phase was taken into account, PVT increased for a more flexed elbow. This probably has to do with the fact that for higher modeled EF, the EF angle right before MER is closer to 90°, resulting in the highest angular deceleration. This result opposes our hypothesis that EF angles above 90° would lead to relatively lower PVT, as we did not take elbow extension into account when we formed the hypothesis. Once again we see that when we simplify the complex pitching movement in order to intuitively understand how high valgus torques develop, accuracy is easily lost.

In conclusion, CoM accelerations of the forearm/hand segment are partly caused by the external rotation deceleration. Secondly, the assumption of a constant EF angle, while the elbow is actually extending in the cocking phase, is an oversimplification that has a huge impact on the results. Therefore, the results from the dynamic EF input are most reliable. These results suggested that higher Elbow Flexion leads to increased PVT and higher External Rotation angle leads to decreased PVT.

Elbow Flexion The shifted Elbow Flexion simulation method (which changed the EF angle at ball release as well as PVT), showed big increases in ball velocity for a more flexed elbow. The scaled method (which kept the EF angle at ball release the same) resulted in a fairly constant ball velocity. The difference might come from the fact that in case of the first method, the elbow is more flexed in the acceleration phase, which makes the internal rotation of the arm more effective. If pitchers are capable of maintaining a higher EF angle throughout the cocking and acceleration phase, the simulations show that this is preferred as it leads to significant ball velocity changes. As EF torque did not change significantly, the model would suggest that this is possible. However, elbow extension in the acceleration phase is presumably a result of velocity-dependent torques induced by the kinetic chain and not by (muscle) torques around the joint itself (Hirashima et al., 2008). It is therefore questionable whether pitchers can consciously influence the EF angle in the acceleration phase. Assuming that the pitchers always extend their elbow fully at ball release (scaled EF simulation), the results showed that pitchers do not have to give in on ball velocity significantly if they want to achieve lower PVT. For most pitchers in this study, the simulations showed that this could be done by extending the elbow more in the cocking phase, which is in line with the results from the two-segment model. However, this was not the case for all subjects.

Escamilla et al. (2002) reported that a high velocity pitch group had a more flexed elbow at ball release, which agrees with our findings. Aguinaldo and Chambers (2009) reported a negative correlation between EF and PVT (R=-0.36), contradictory to the results of all three research methods in this study. In their study, the mean Elbow Flexion at PVT was 43°, which was lower (more extended) than in the data (85.9°) and models ($60° - 110°$) of our study. Furthermore, some of their subjects (14 out of 69) practiced the sidearm technique, in which the arm is more horizontal than in the common overhand or three-quarter delivery style. As they also mentioned, a more extended elbow leads to a smaller moment arm about the internal rotation axis (rotational inertia), but a larger moment arm about the thorax rotation axis (leading to higher forward accelerations - translational inertia). It is likely that for EF angles this low, the translational inertia mechanism is dominant, indeed leading to higher PVT with a more extended elbow (lower EF angles). Thus, from the differences between the results of our study and Aguinaldo and Chambers (2009), we hypothesize that the effect of Elbow Flexion on PVT is dependent on the player's pitching style.

External Rotation For the biggest group of pitchers (6/12), the simulations showed a decreased PVT when the arm was further externally rotated, which agrees with the results of the two-segment model. However, for the others the effects were diverse. This shows that the effect of ER on PVT is very personal and might be dependent on other factors in the pitcher's technique. The same accounts for the influence on ball velocity, although the majority showed an optimal External Rotation angle. The changes in ball velocity remained small for most pitchers. Thus, the simulations showed that a decrease in PVT is not necessarily linked to a decrease in ball speed.

However, the statistical analysis did show a significant trend of higher ER leading to decreased ball velocity. Contrarily, Escamilla et al. (2002) reported that a high velocity pitching group had higher MER angles than a low velocity group. The statistical power of their study (19 subjects) was not much higher than in ours. They argued that pitchers with higher MER had a greater arc over which the ball could be accelerated. This assumes that when the MER angle changes, the ER angle at ball release remains the same, while our simulations assumed a shift of that arc. Clearly, the angle as well as angular acceleration play a role, but it is unclear whether the MER angle and the range of ER in the acceleration phase are really related. Thus, the effect of ER on ball velocity is still debated.

Aguinaldo and Chambers (2009) and Sabick et al. (2004) reported positive correlations between MER and PVT (R=0.55 and R=0.65), indicating that high MER could be harmful. Their findings do not agree with the results of our two-segment model and simulations. First of all, Aguinaldo et al. and Sabick et al. did not correct for ball velocity. Their subjects with higher MER might also have experienced a higher ball velocity. Secondly, in our models, we kept the angular accelerations of ER the same as in the original data. Subjects in their studies who showed higher MER might have also experienced a higher External Rotation deceleration - an expected effect if they started externally rotating from a similar starting position (which is not certain). The authors of these studies did not present any thought on why PVT could have increased with increasing MER. Aguinaldo and Chambers even regarded it as an expected trend - "... higher shoulder external rotation is expected to increase elbow valgus", while referring to the previously mentioned study of Sabick et al. and an article by Fleisig et al. (1995). Although Fleisig's work, relating pitching biomechanics to upper extremity injury, is an important piece in pitching literature, this is an unjust reference as the article does not mention anything about the role of MER angle on valgus torque or elbow injury. Following the results of our study, we believe that this discussion should be re-opened.

4.2 Limitations

Two-segment model In the previous parts of this paper, we discussed the trends of PVT in the two-segment model, but we did not refer to the absolute PVT values. The reason for this is that these values were not realistic, due to some movements being suppressed in the model for simplification purposes. Although the absolute PVT values were not realistic, the results of the two-segment model were still valuable in terms of analyzing the trends.

An important example of a suppressed movement is the elbow valgus rotation. Non-zero valgus angles were found in the data, but not input to the model. Therefore, the internal joint torques turn out higher. As a matter of fact, no such valgus rotation is actually happening in the joint, this is merely a result of the simplification of the rotation axes of the elbow. It assumes a perfectly outlined hinge, which is not the case in reality. The abduction angle is a projection of the carrying angle that changes with elbow flexion (Van Roy et al., 2005). Furthermore, as mentioned in the introduction, the rough estimation of the flexion axis might have led to projection of flexion/extension rotations on the valgus axis.

For most pitchers, we saw that the trends in the results of the two-segment model agreed with those of the simulations. This makes sense as the input of the two-segment model, although simplified, was based on the average of the pitchers. However, as mentioned before, different results in other studies could be caused by differences in pitching technique. The two-segment model is a useful tool to gain insight in factors affecting PVT. But for pitchers with very different technique from the ones in this study (so different input), the variables (EF and ER) might have a different effect on PVT.

Simulations Performance was taken into account by correcting for, or at least considering, changes in ball velocity. Correcting for ball velocity in the simulations of External Rotation did not show to be feasible. Multiple methods were tried, but these changes had unrealistic effects on the valgus torque, changing its course over time drastically. Additionally, the effect of ER on ball velocity was different for all pitchers, so no unified method would be possible. Scaling of the acceleration phase for each pitcher was not regarded as an option, as a preliminary analysis showed only little variation in the duration of the pitching phases within and between pitchers. Partly because of this, the influence of ER on ball velocity is still debatable.

General The ongoing question is whether the modeled changes in the data (Table 2) are realistic and could be brought into practice. Although performance was taken into account by evaluating the influence on ball velocity, changing the EF and ER angles might result in a poorly aimed ball. Additionally, the range of motion in the joints of a pitcher could be unsuited for these changes. Pitchers should be careful not to sacrifice the safety of their shoulder joint by trying to reach a higher MER. Personal communication with T. Sgroi (doctorate in physical therapy, working with doctors and baseball coaches extensively) revealed that most pitchers probably already Externally Rotate to their full potential and that this movement is expected to be a result of the kinetic chain. As mentioned before, Hirashima et al. (2008) mentioned the same about elbow extension. It is therefore questionably whether pitcher have conscious control over their ER and EF angle.

A drawback of the two-segment model as well as the simulations is that they do not take into account compensatory movements. Along with changes in EF and ER, it might be necessary for pitchers to change other aspects in their movement. However, this methodology was chosen despite that, because of the added value that it ensures causality.

4.3 Recommendations

The goal of this study was to find out how Elbow Flexion and arm External Rotation influence Peak Valgus Torque as well as ball velocity. The results showed that high PVT was related to high EF angles and low ER angles, while ball velocity was not necessarily affected by these variables. As mentioned, pitchers might not be able to consciously influence the EF and ER angles as they are presumed to be results of the kinetic chain. Future research can focus on answering that question and trying to find out what movements down the kinetic chain could lead to these changes.

This study showed that lower valgus torques due to changes in EF or ER are not necessarily accompanied by lower ball speeds. Thus, research that looks to decrease these joint torques proves to be useful. Although correcting for ball velocity was not possible for all parts of this study, this is the first study relating technique explicitly to valgus torque as well as ball velocity. We underline the importance of this for further research, in order to provide information that is relevant for the pitching practice.

As the results differed between pitchers and between studies, other pitching technique factors probably influence the effect of EF and ER on PVT. Delivery style might be a way to characterize some of these differences. The most practiced delivery style is the three-quarter technique (Whiteley, 2007). Compared to the three-quarter and overhand technique, sidearm pitching shows a more extended elbow and additionally a less sideflexed (more upright) thorax. This might lead to the forearm experiencing relatively more forward acceleration and less angular acceleration. Therefore, we recommend that more research is carried out to investigate whether delivery style influences valgus torque and the effect of EF and ER on it. Additionally, a personal approach could be interesting. This could for instance be done by applying a fast inverse dynamics algorithm to accelerometer/gyrometer measurements.

To gain more insight in the most beneficial pitching technique in terms of low torques and high ball velocity, future research could look into forward dynamic optimization techniques. Using a rigid body model with boundary conditions such as minimal/maximal joint angles and torques, the movement could be optimized to a cost function that includes ball velocity and torque. Anderson et al. (2007) have developed a model that estimates joint torques as a function of joint angle and angular velocity, which could (once applied to the upper limb) eliminate the need for a muscle model. One of the main challenges associated of a forward dynamic optimization method is to model and optimize the direction of the ball at release, for instance by including an interaction between the hand/fingers and the ball, or by defining an end position of the hand. Additionally, the more degrees of freedom the models holds, the harder it is to distinguish whether a local or global optimum is found. However, if the challenges can be dealt with, forward dynamic optimization could lead to the advantage of providing a movement - possibly out-of-the-box - that optimizes for some of the main objectives of a pitcher: high velocity and low injury risk.

The main motivation for this research was the high incidence of UCL injury. Although a relationship between valgus torque and force on the UCL evidently exists, it is not clear to what extent valgus torque can directly represent UCL stress. Additionally, elbow distraction force was not considered in this study. We hypothesize that distraction forces stress the UCL and additionally decrease the contribution of a contact force between the ulna and humerus to elbow valgus stability. A detailed model of the elbow joint structures, including the UCL, could give more insight in this issue. However, the error in motion data (e.g. due to skin movement) is bigger than the strains a ligament like the UCL could bear. This would lead to large calculated length changes and thereby huge forces stressing the ligament (Pronk et al., 1993). Although global optimization of the kinematic data could diminish this effect, inverse dynamic modeling is not ideal for this purpose. Again, forward dynamic modeling could be an outcome. This could be possible with the Delft Shoulder and Elbow Model (DSEM) (Nikooyan et al., 2011). In that case assumptions should be made on the origo, insertion and lines of action of the UCL as well as its dynamic behavior (using maximum strain and stress estimations and stress-strain curve shape assumptions).

5 Conclusion

This study provided a more in-depth understanding of the factors that play a role in the development of high valgus torques in pitching. We hypothesized that valgus torque is mainly generated by external rotation deceleration and forward acceleration of the forearm CoM. It appeared that these forearm accelerations were not only caused by full body accelerations, thorax axial rotations and shoulder horizontal abduction, but also by external rotation deceleration and elbow extension acceleration. Therefore, assuming a constant elbow flexion in the cocking phase was concluded to be an oversimplification of the two-segment model.

Generally, we found that higher humerothoracic External Rotation angles led to decreased Peak Valgus Torque, in line with our hypothesis. As previous research reported opposite results and did not offer an interpretation of them, we believe this discussion should be re-opened. Previous studies reported an increase of ball velocity with higher ER, while our statistical analysis indicated a decrease and the simulations showed differing results between subjects. Therefore, this relationship is still debated, but we can conclude that optimizing the ER angle to decrease PVT does not necessarily lead to a negative effect on performance.

Higher Elbow Flexion appeared to cause higher Peak Valgus Torques. However, if pitchers are able to increase their flexion angle at ball release as well as before MER, this is recommended as it showed to increase ball velocity significantly. Otherwise, this study showed that extending the elbow more (lower EF) can lower peak valgus torque while ball velocity is not necessarily affected.

Future research may look at forward dynamic modeling that optimizes for low peak valgus torque and high ball velocity. As the influence of EF and ER varied between pitchers and studies, the influence of different delivery styles could also be subject to research. Lastly, specific research into the UCL and the relationship between valgus torque and UCL stress is recommended.

This research provided insights that can help to prevent injuries in pitching. Although pitchers might not be able to directly influence the Elbow Flexion and External Rotation angles in their pitch, the results of this study suggest that some pitchers (e.g. who have a relatively low external rotation range of motion) might be more prone to high valgus torques and thus to elbow injury than others. Additionally, pitchers who have a decreased maximal elbow extension might be able to throw faster. Further research could study how movements down the kinetic chain could lead to beneficial changes in joint angles.

Bibliography

Aguinaldo, A. L. and H. Chambers
2009. Correlation of throwing mechanics with elbow valgus load in adult baseball pitchers. *The American journal of sports medicine*, 37(10):2043–2048.

Anderson, D. E., M. L. Madigan, and M. A. Nussbaum
2007. Maximum voluntary joint torque as a function of joint angle and angular velocity: model development and application to the lower limb. *Journal of biomechanics*, 40(14):3105–3113.

Anz, A. W., B. D. Bushnell, L. P. Griffin, T. J. Noonan, M. R. Torry, and R. J. Hawkins
2010. Correlation of torque and elbow injury in professional baseball pitchers. *The American journal of sports medicine*, 38(7):1368–1374.

Cain, E. L., J. R. Dugas, R. S. Wolf, and J. R. Andrews
2003. Elbow injuries in throwing athletes: a current concepts review. *The American journal of sports medicine*, 31(4):621–635.

Conte, S., R. K. Requa, and J. G. Garrick
2001. Disability days in major league baseball. *The American journal of sports medicine*, 29(4):431–436.

Conte, S. A., G. S. Fleisig, J. S. Dines, K. E. Wilk, K. T. Aune, N. Patterson-Flynn, and N. ElAttrache
2015. Prevalence of ulnar collateral ligament surgery in professional baseball players. *The American journal of sports medicine*, 43(7):1764–1769.

Dumas, R., R. Aissaoui, and J. A. de Guise
2004. A 3d generic inverse dynamic method using wrench notation and quaternion algebra. *Computer methods in biomechanics and biomedical engineering*, 7(3):159–166.

Dumas, R., L. Cheze, and J.-P. Verriest
2007. Adjustments to mcconville et al. and young

et al. body segment inertial parameters. *Journal of biomechanics*, 40(3):543–553.

Erickson, B. J., B. U. Nwachukwu, S. Rosas, W. W. Schairer, F. M. McCormick, B. R. Bach Jr, C. A. Bush-Joseph, and A. A. Romeo
2015. Trends in medial ulnar collateral ligament reconstruction in the united states: a retrospective review of a large private-payer database from 2007 to 2011. *The American journal of sports medicine*, 43(7):1770–1774.

Escamilla, R., G. Fleisig, S. Barrentine, J. Andrews, and C. Moorman III
2002. Baseball: Kinematic and kinetic comparisons between american and korean professional baseball pitchers. *Sports Biomechanics*, 1(2):213–228.

Fleisig, C. S., R. F. Escamilla, J. R. Andrews, T. Matsuo, and S. W. Barrentine
1996. Kinematic and kinetic comparison between baseball pitching and football passing. *Journal of Applied Biomechanics*, 12(2).

Fleisig, G. S., J. R. Andrews, C. J. Dillman, and R. F. Escamilla
1995. Kinetics of baseball pitching with implications about injury mechanisms. *The American journal of sports medicine*, 23(2):233–239.

Fortenbaugh, D., G. S. Fleisig, and J. R. Andrews
2009. Baseball pitching biomechanics in relation to injury risk and performance. *Sports health*, 1(4):314–320.

Gasparutto, X., E. van der Graaff, F. van der Helm, and H. Veeger
2016. Elite athlete motor and loading actions on the upper limb in baseball pitching. *Procedia Engineering*, 147:181–185.

Hariri, S. and M. R. Safran
2010. Ulnar collateral ligament injury in the overhead athlete. *Clinics in sports medicine*, 29(4):619–644.

Hirashima, M., K. Yamane, Y. Nakamura, and T. Ohtsuki
2008. Kinetic chain of overarm throwing in terms of joint rotations revealed by induced acceleration analysis. *Journal of biomechanics*, 41(13):2874–2883.

Huang, Y.-H., T.-Y. Wu, K. E. Learman, and Y.-S. Tsai
2010. A comparison of throwing kinematics between youth baseball players with and without a history of medial elbow pain. *Chin J Physiol*, 53(3):160–166.

Hurd, W. J., K. R. Kaufman, and N. S. Murthy
2011. Relationship between the medial elbow adduction moment during pitching and ulnar collateral ligament appearance during magnetic resonance imaging evaluation. *The American journal of sports medicine*, 39(6):1233–1237.

Kooima, C. L., K. Anderson, J. V. Craig, D. M. Teeter, and M. van Holsbeeck
2004. Evidence of subclinical medial collateral ligament injury and posteromedial impingement in professional baseball players. *The American journal of sports medicine*, 32(7):1602–1606.

Lyman, S., G. S. Fleisig, J. W. Waterbor, E. M. Funkhouser, L. Pulley, J. R. Andrews, E. D. Osinski, and J. M. Roseman
2001. Longitudinal study of elbow and shoulder pain in youth baseball pitchers. *Medicine and science in sports and exercise*, 33(11):1803–1810.

Matsuo, T., G. S. Fleisig, N. Zheng, and J. R. Andrews
2006. Influence of shoulder abduction and lateral trunk tilt on peak elbow varus torque for college baseball pitchers during simulated pitching. *Journal of applied biomechanics*, 22(2):93–102.

Moen, E. L., C. J. Fricano-Kugler, B. W. Luikart, and A. J. O'Malley
2016. Analyzing clustered data: why and how to account for multiple observations nested within a study participant? *Plos one*, 11(1):e0146721.

Nikooyan, A. A., H. Veeger, E. Chadwick, M. Praagman, and F. C. van der Helm
2011. Development of a comprehensive musculoskeletal model of the shoulder and elbow. *Medical & biological engineering & computing*, 49(12):1425–1435.

Pronk, G., F. Van der Helm, and L. Rozendaal
1993. Interaction between the joints in the shoulder mechanism: the function of the costoclavicular, conoid and trapezoid ligaments. *Proceedings of the Institution of Mechanical Engineers, Part H: Journal of Engineering in Medicine*, 207(4):219–229.

Sabick, M. B., M. R. Torry, R. L. Lawton, and R. J. Hawkins
2004. Valgus torque in youth baseball pitchers: a biomechanical study. *Journal of Shoulder and Elbow Surgery*, 13(3):349–355.

Safran, M., C. S. Ahmad, and N. S. Elattrache
2005. Ulnar collateral ligament of the elbow. *Arthroscopy: The Journal of Arthroscopic & Related Surgery*, 21(11):1381–1395.

Van Roy, P., J. Baeyens, D. Fauvart, R. Lanssiers, and J. Clarijs
2005. Arthro-kinematics of the elbow: study of the carrying angle. *Ergonomics*, 48(11-14):1645–1656.

Werner, S. L., G. S. Fleisig, C. J. Dillman, and J. R. Andrews
1993. Biomechanics of the elbow during baseball pitching. *Journal of Orthopaedic & Sports Physical Therapy*, 17(6):274–278.

Werner, S. L., T. A. Murray, R. J. Hawkins, and T. J. Gill
2002. Relationship between throwing mechanics and elbow valgus in professional baseball pitchers. *Journal of shoulder and elbow surgery*, 11(2):151–155.

Whiteley, R.
2007. Baseball throwing mechanics as they relate to pathology and performance—a review. *J Sports Sci Med*, 6(1):1–20.

Wu, G., S. Siegler, P. Allard, C. Kirtley, A. Leardini, D. Rosenbaum, M. Whittle, D. D D'Lima, L. Cristofolini, H. Witte, et al.
2002. Isb recommendation on definitions of joint coordinate system of various joints for the reporting of human joint motion—part i: ankle, hip, and spine. *Journal of biomechanics*, 35(4):543–548.

Wu, G., F. C. Van der Helm, H. D. Veeger, M. Makhsous, P. Van Roy, C. Anglin, J. Nagels, A. R. Karduna, K. McQuade, X. Wang, et al.
2005. Isb recommendation on definitions of joint coordinate systems of various joints for the reporting of human joint motion—part ii: shoulder, elbow, wrist and hand. *Journal of biomechanics*, 38(5):981–992.

Zheng, N., G. S. Fleisig, S. Barrentine, and J. R. Andrews
2004. Biomechanics of pitching. *Biomedical engineering principles in sports*, Pp. 209–256.

Appendices

A Markers, SCS and JCS

Active infrared markers were placed on anatomical landmarks on the full body of the subjects. The markers that were used for the dynamics are described below per segment. For phase estimation, the knee and ankle joint centers were used: the knee joint center is at the midpoint of the lateral and medial femoral epicondyle markers (LFE and MFE) and the ankle joint center is at the midpoint of the lateral and medial malleoli (LM and MM).

Segment coordinate systems

Thorax

The y-axis points from the midpoint between the Xiphoid Process (PX) and the 8th thoracic vertebra (T8) to the midpoint between Incisura Jugularis (IJ) and the 7th cervical vertebra (C7). The temporary z-axis is normal to the plane spanned by the PX-T8 midpoint, IJ, and C7 (pointing to the right). The x-axis is orthogonal to the plane spanned by y_t and z_{temp} (pointing forward) and the final z-axis is orthogonal to the y_t and x_t axes.

$$y_t = \frac{\frac{1}{2}(IJ+C7)-\frac{1}{2}(PX+T8)}{||\frac{1}{2}(IJ+C7)-\frac{1}{2}(PX+T8)||} \tag{3}$$

$$z_{temp} = \frac{IJ-\frac{1}{2}(PX+T8)\times C7-\frac{1}{2}(PX+T8)}{||IJ-\frac{1}{2}(PX+T8)\times C7-\frac{1}{2}(PX+T8)||} \tag{4}$$

$$x_t = y_t \times z_{temp} \tag{5}$$

$$z_t = x_t \times y_t \tag{6}$$

The origin of the thorax SCS is in the IJ.

$${}_gR_t = [x_t \quad y_t \quad z_t] \tag{7}$$

$${}_gT_t = \begin{bmatrix} & {}_gR_t & & IJ \\ 0 & 0 & 0 & 1 \end{bmatrix} \tag{8}$$

Right upper arm

The position of the gleno-humeral joint (GH) is estimated from regression equations (Dumas et al., 2007). The elbow joint center (EJC) is the midpoint between the medial and lateral humeral epicondyles (MHE and LHE). The y-axis points from EJC to GH. The temporary z-axis points from the RMHE to RLHE. The x-axis is orthogonal to the plane spanned by y_{ua} and z_{temp} (pointing forward) and the final z-axis is orthogonal to the y_{ua} and x_{ua} axes.

$$y_{ua} = \frac{GH-EJC}{||GH-EJC||} \tag{9}$$

$$z_{temp} = \frac{LHE-MHE}{||LHE-MHE||} \tag{10}$$

$$x_{ua} = y_{ua} \times z_{temp} \tag{11}$$

$$z_{ua} = x_{ua} \times y_{ua} \tag{12}$$

The origin of the upper arm SCS is in GH.

$${}_gR_{ua} = [x_{ua} \quad y_{ua} \quad z_{ua}] \tag{13}$$

$${}_gT_{ua} = \begin{bmatrix} & {}_gR_{ua} & & GH \\ 0 & 0 & 0 & 1 \end{bmatrix} \tag{14}$$

Right forearm

The y-axis points from the ulnar styloid (US) to EJC. The temporary z-axis points from US to the radial styloid (RS). The x-axis is orthogonal to the plane spanned by y_{fa} and z_{temp} (pointing forward) and the final z-axis is orthogonal to the y_{fa} and x_{fa} axes.

$$y_{fa} = \frac{EJC - US}{||EJC - US||} \tag{15}$$

$$z_{temp} = \frac{RS - US}{||RS - US||} \tag{16}$$

$$x_{fa} = y_{fa} \times z_{temp} \tag{17}$$

$$z_{fa} = x_{fa} \times y_{fa} \tag{18}$$

The origin of the forearm SCS is in the EJC.

$${}_gR_{fa} = \begin{bmatrix} x_{fa} & y_{fa} & z_{fa} \end{bmatrix} \tag{19}$$

$${}_gT_{fa} = \begin{bmatrix} & {}_gR_{fa} & & EJC \\ 0 & 0 & 0 & 1 \end{bmatrix} \tag{20}$$

Right hand

The wrist joint center (WJC) is estimated as the midpoint of the US and RS. The y-axis points from right hand middle finger interphalangeal joint (RHIP3) to WJC. The temporary z-axis points from US to the radial styloid (RS). The x-axis is orthogonal to the plane spanned by y_h and z_{temp} (pointing forward) and the final z-axis is orthogonal to the y_h and x_h axes.

$$y_h = \frac{WJC - RHIP3}{||WJC - RHIP3||} \tag{21}$$

$$z_{temp} = \frac{RS - US}{||RS - US||} \tag{22}$$

$$x_h = y_h \times z_{temp} \tag{23}$$

$$z_h = x_h \times y_h \tag{24}$$

The origin of the hand SCS is in the WJC.

$${}_gR_h = \begin{bmatrix} x_h & y_h & z_h \end{bmatrix} \tag{25}$$

$${}_gT_h = \begin{bmatrix} & {}_gR_h & & WJC \\ 0 & 0 & 0 & 1 \end{bmatrix} \tag{26}$$

Joint coordinate systems

The humerothoracic JCS is defined as the rotation of the upper arm relative to the thorax:

$${}_tR_{ua} = {}_gR_t^{-1} \, {}_gR_{ua} \tag{27}$$

The elbow JCS is defined as the rotation of the forearm relative to the upper arm:

$${}_{ua}R_{fa} = {}_gR_{ua}^{-1} \, {}_gR_{fa} \tag{28}$$

The wrist JCS is defined as the rotation of the hand relative to the forearm:

$${}_{fa}R_h = {}_gR_{fa}^{-1} \, {}_gR_h \tag{29}$$

B Angles to transformation matrices

Similar methods were used in the two-segment model and the simulations. The joint angles θ_1, θ_2 and θ_3 - whether their values were defined or adjusted from original data - were used to calculate the joint rotation matrices and then the segment transformation matrices for every frame. The latter were transformed to quaternions and subsequently used as input to the inverse dynamics equations.

The rotation matrix for the joint between proximal segment p (e.g. thorax) and distal segment d (e.g. upper arm) can be constructed for any Euler sequence (1,2,3) with the corresponding angles (θ_1, θ_2, θ_3) as follows:

$$_pR_d = R_1 R_2 R_3 \tag{30}$$

Where R_i is the rotation matrix about the x, y or z-axis. This depends on the sequence: for the humerothoracic JCS $_pR_d = R_y R_x R_y$ while for the elbow and wrist $_pR_d = R_z R_x R_y$. In all cases

$$R_x = \begin{bmatrix} 1 & 0 & 0 \\ 0 & \cos(\theta_x) & -\sin(\theta_x) \\ 0 & \sin(\theta_x) & \cos(\theta_x) \end{bmatrix} \tag{31}$$

$$R_y = \begin{bmatrix} \cos(\theta_x) & 0 & \sin(\theta_x) \\ 0 & 1 & 0 \\ -\sin(\theta_x) & 0 & \cos(\theta_x) \end{bmatrix} \tag{32}$$

$$R_z = \begin{bmatrix} \cos(\theta_x) & -\sin(\theta_x) & 0 \\ \sin(\theta_x) & \cos(\theta_x) & 0 \\ 0 & 0 & 1 \end{bmatrix} \tag{33}$$

The rotation matrix of the distal segment (e.g. upper arm) with respect to the global coordinate system (g) is subsequently calculated:

$$_gR_d = {_gR_p} \cdot {_pR_d} \tag{34}$$

In this, $_gR_p$ is the rotation matrix of the proximal segment (e.g. thorax) with respect to the global coordinate system. In the two-segment model the thorax rotation matrix was defined as either upright, forward facing and stationary (all thorax angles 0°) or axially rotating (all thorax angles 0° except for axial rotation). In the simulations, the thorax rotation matrix was simply taken from the original data.

The transformation matrix $_gT_d$ of the distal segment (e.g. upper arm) is calculated using the joint center position p_{jc}:

$$_gT_d = \begin{bmatrix} & {_gR_d} & & p_{jc} \\ 0 & 0 & 0 & 1 \end{bmatrix} \tag{35}$$

In the two-segment model, p_{jc} for the upper arm was defined as $[\ 0 \quad 0 \quad 0\ ]^T$ or changing between frames, according to average timeseries. In the simulations, p_{jc} was taken from the original transformation matrix.

Subsequently, the position of the adjacent joint centre (e.g. elbow) can be calculated by using its position in the segment coordinate system:

$$^gp_{jc2} = {_gT_d^{-1}} \cdot {^Lp_{jc}} \tag{36}$$

In the two-segment model, $^Lp_{jc} = [\ 0 \quad -l \quad 0\ ]^T$ using the segment length l. In the simulations, the local position of the original data was used.

For the forearm-hand segment in the two-segment model and the forearm segment in the simulations, the steps in Equations (30-35) were repeated. For the hand segment in the simulations, the rotation matrix of the wrist joint was taken from the original data

$$_pR_d = {_gR_p^{-1}} \cdot {_gR_d} \tag{37}$$

and then the steps in Equations (34-35) were repeated.

C Joint kinematics

This appendix shows the mean ± Standard Deviation (SD) over all pitches for thorax angles with respect to the global coordinate system, shoulder (gleno-humeral joint) displacement, shoulder (humerothoracic) angles and elbow joint angles. The input of the two-segment model is based on these values between FC and MER.

Additionally, the mean ± SD of the CoM is plotted below, to be able to compare them to the outcomes of the two-segment model.

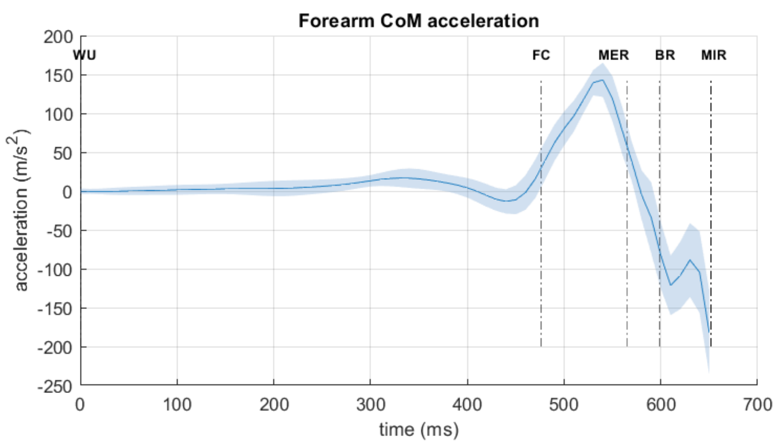

Figure 16: Forearm Center of Mass (CoM) mean ± SD forward acceleration in the global frame.

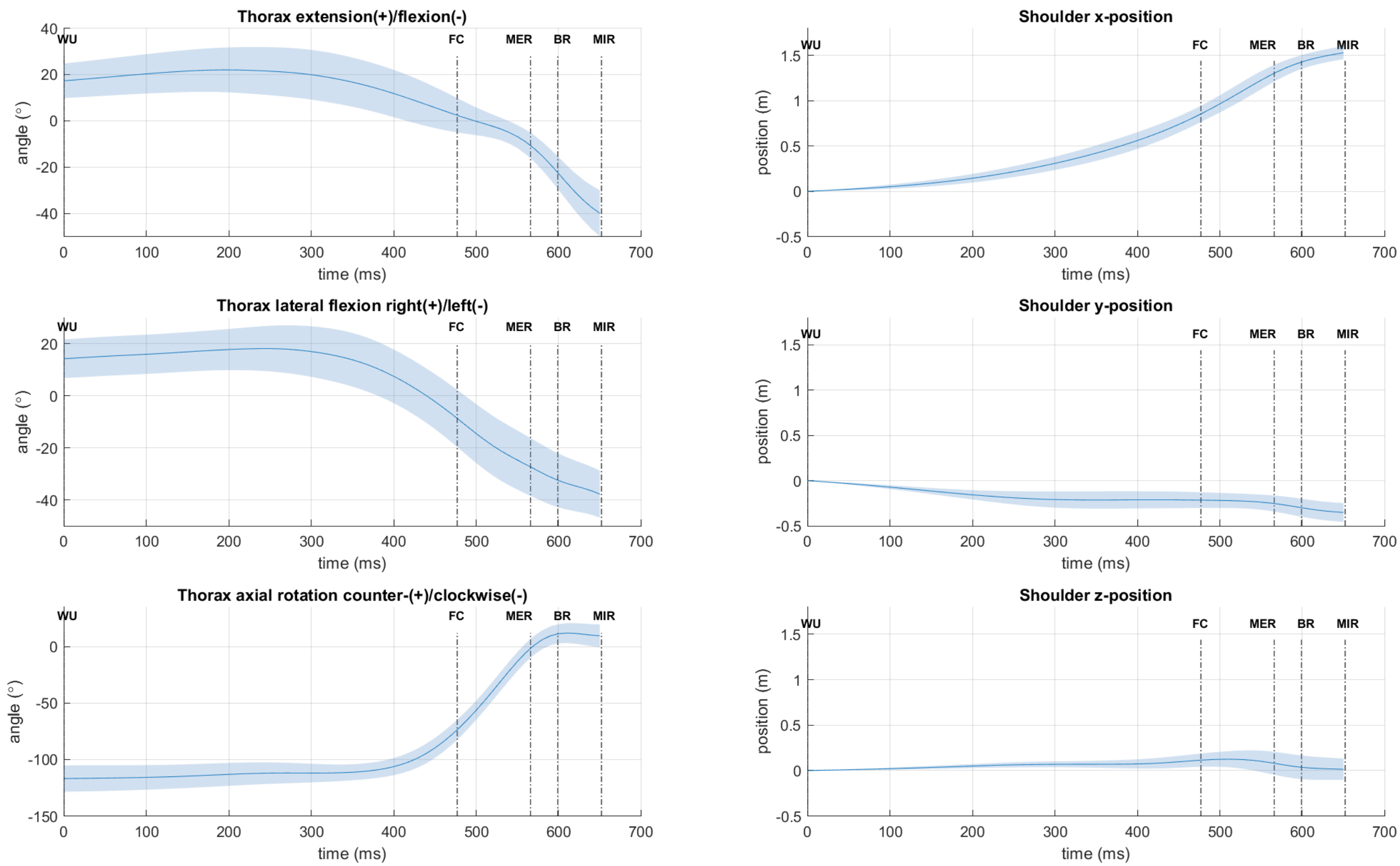

Figure 17: Thorax mean ± SD Euler angles over all 29 pitches & shoulder mean ± SD position in the global coordinate system over all 29 pitches, relative to the WU position.

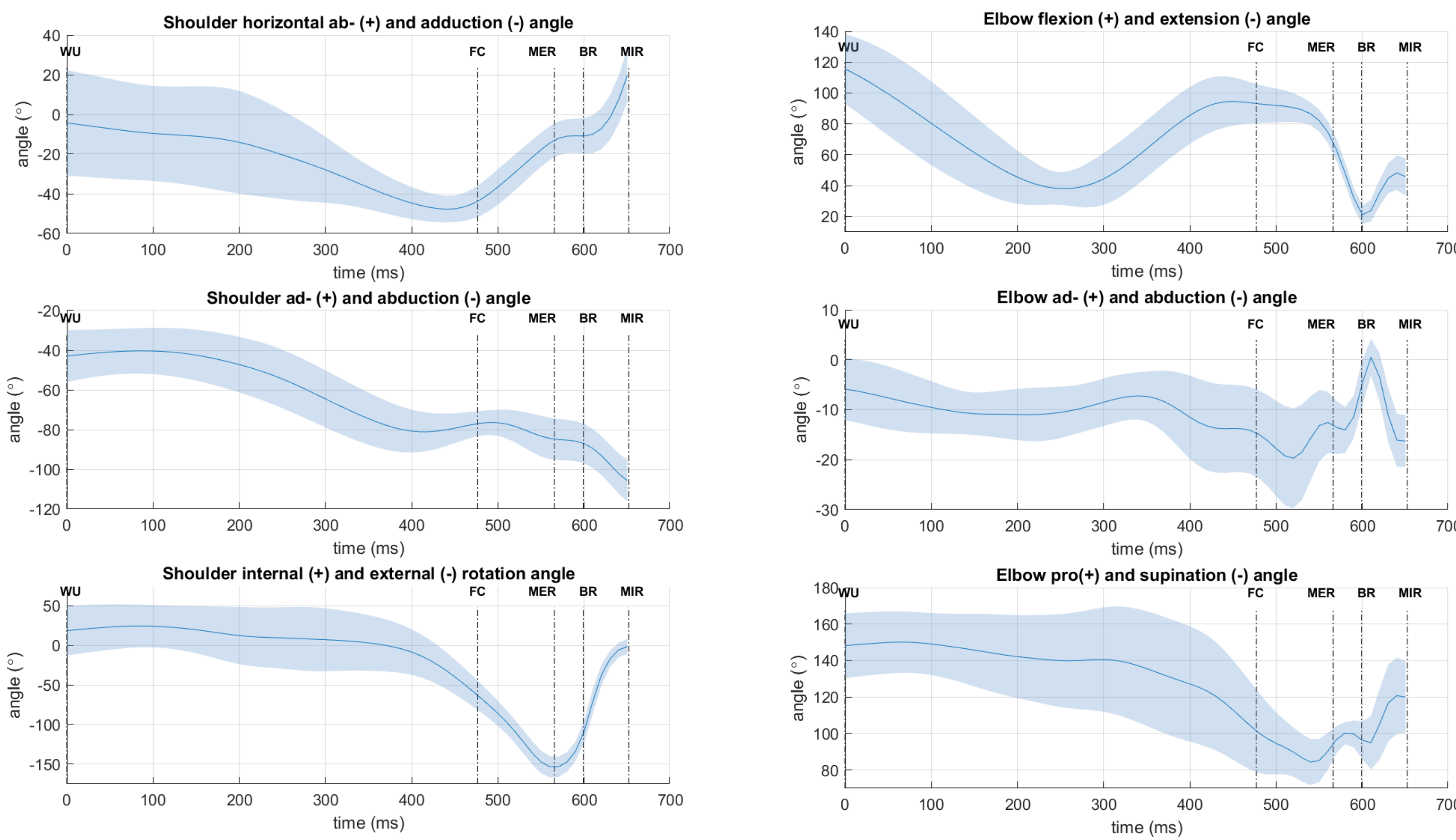

Figure 18: Shoulder and elbow mean ± SD joint Euler angles over all 29 pitches.

D Simulations: scaled EF

For the scaling of the EF angle in the simulations, the following method was used.

For the frames i before minimum EF angle (minEF) and after BR, the EF angle was defined as

$$EF(i) = EF_0(i) \tag{38}$$

At PVT, EF was shifted with the defined ΔEF:

$$EF(PVT) = EF_0(PVT) + \Delta EF \tag{39}$$

Leading up to and after PVT, the angle was scaled smoothly. Between minEF and PVT, this done with a scaling factor f_1 from 0 to 1:

$$f_1(i) = \frac{i - minEF}{PVT - minEF} \tag{40}$$

$$EF(i) = EF_0(i) + f1(i) \cdot \Delta EF \tag{41}$$

Between PVT and BR, the angle was scaled with a factor from 1 to 0 (f_2):

$$f_2(i) = 1 - \frac{i - PVT}{BR - PVT} \tag{42}$$

$$EF(i) = EF_0(i) + f2(i) \cdot \Delta EF \tag{43}$$

These changes would intuitively lead to increased elbow flexion torques. Therefore in Figure 19 the peak elbow flexion torque is plotted as a function of the elbow flexion angle, to show deviations of EFT from the original data. Elbow flexion torque was only increased significantly for one pitcher.

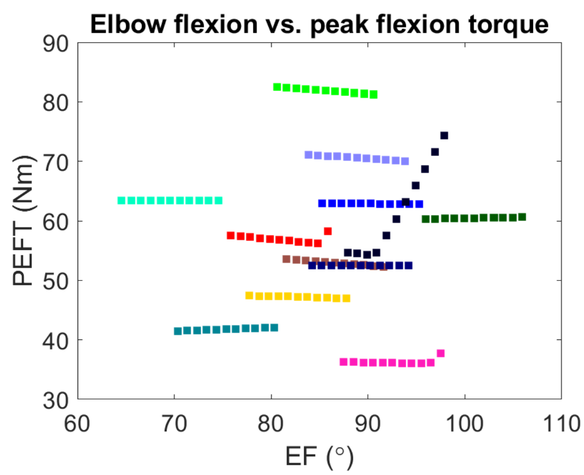

Figure 19: Simulations: effect of scaled Elbow Flexion (EF) (value at original time of PVT) on peak elbow flexion torque. Each color represents simulated values for one pitcher.

NB: The scaling method was chosen because the time series of EF differ a lot between pitchers. All pitchers showed a local minimum of EF somewhere in the stride phase. The example in the paper showed a maximum EF at PVT, but this is not the case for all pitchers.

E EF and ER within/between subject variation

	EF		ER	
Subject	Mean	Diff	Mean	Diff
1	90.3	1.0	-130.4	4.8
2	90.6	3.9	-118.4	7.3
3	82.7	0.0	-111.3	0.0
4	83.4	4.5	-134.4	51.0
5	95.3	11.4	-151.5	23.6
6	88.0	1.6	-160.6	6.8
7	86.6	0.1	-147.4	6.8
8	90.6	4.8	-129.9	31.4
9	96.6	7.3	-145.2	3.7
10	73.5	4.7	-133.7	10.1
11	76.1	1.5	-138.2	6.7
12	90.2	1.9	-132.1	3.5
	Mean	SD	Mean	SD
All	87.0	3.3	136.1	15.0

Table 5: Elbow Flexion (EF) and External Rotation (ER) angles at the instant of Peak Valgus Torque (PVT): within and between subject variation. Diff = the largest difference found between two pitches of the subject. SD = standard deviation.

F Two-segment model: results

This appendix visualizes the effects of the two-segment model inputs on the valgus/varus torque. The movements, variables and outcomes are plotted for three cases (lowest, reference and highest), as well as the forearm forward acceleration.

From left to right:

- The simplified movements: (1) external rotation, (2) horizontal abduction, (3) forward translation and (4) combination. For (1-3) the input of the movement is plotted. For 4, the input is the combination of (1-3) and plotted is the forearm/hand segment CoM position.
- The variable (constant EF, dynamic EF, ER): in blue the original, in yellow the lowest and in red the highest variation.
- Valgus torque time series as a result of the movement and variable.
- Forearm CoM forward acceleration as a result of the movement and variable.

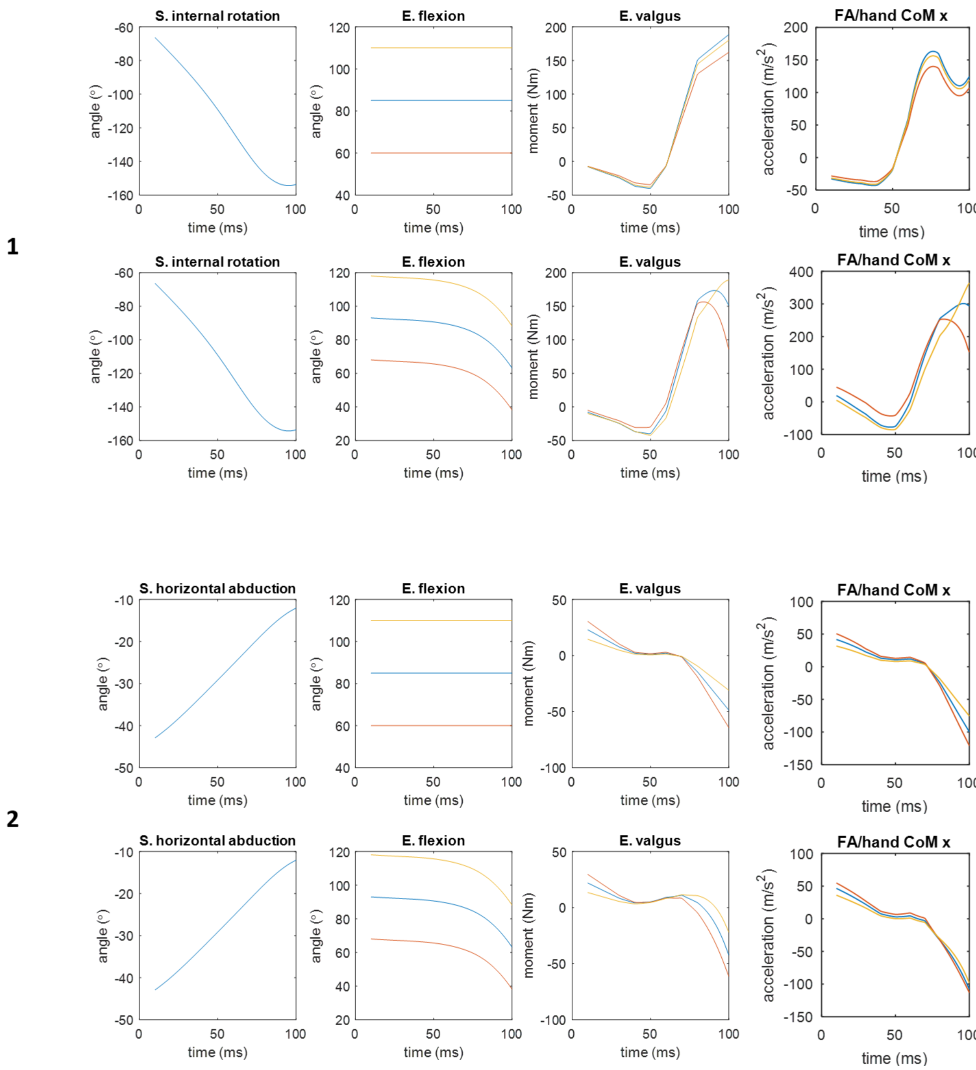

Figure 20: Influence of Elbow Flexion (EF) variations for movements 1 and 2: constant EF (above) and dynamic EF (below).

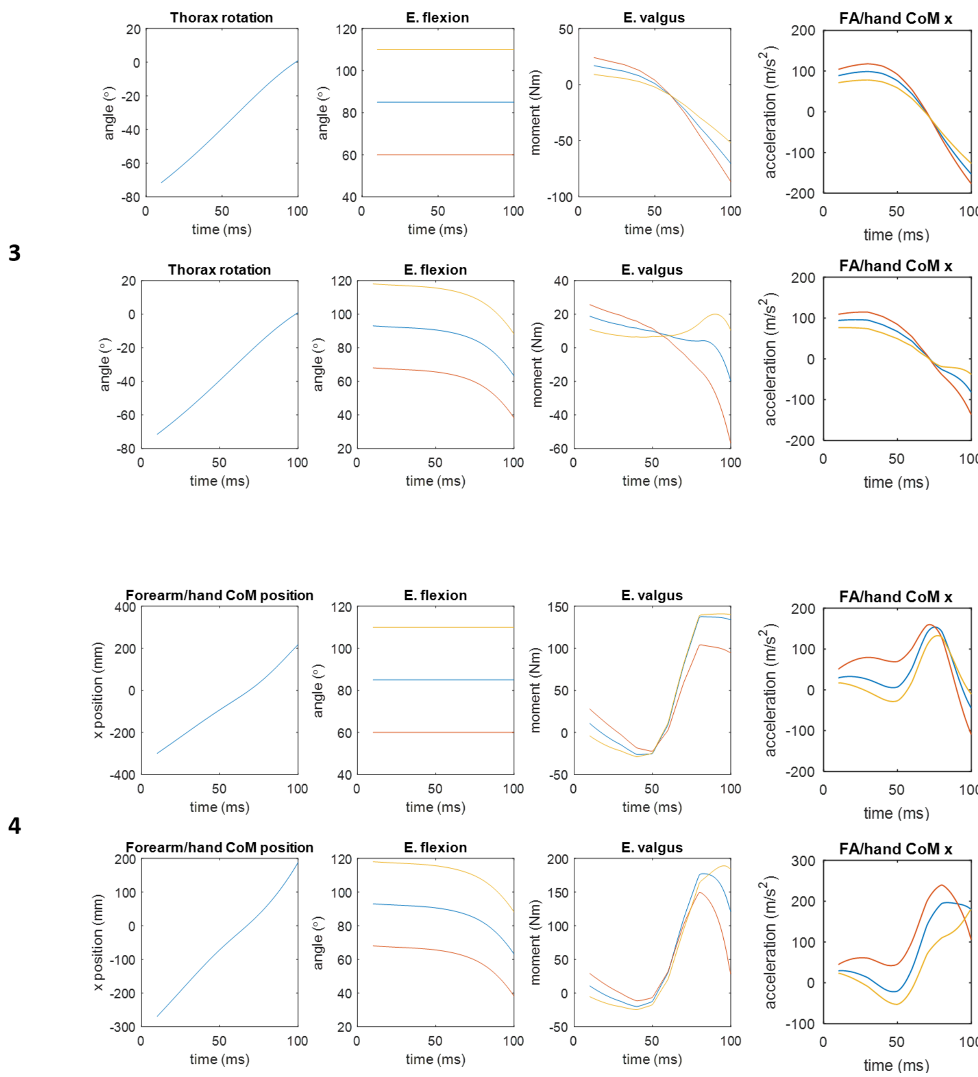

Figure 21: Influence of Elbow Flexion (EF) variations for movements 3 and 4: constant EF (above) and dynamic EF (below).

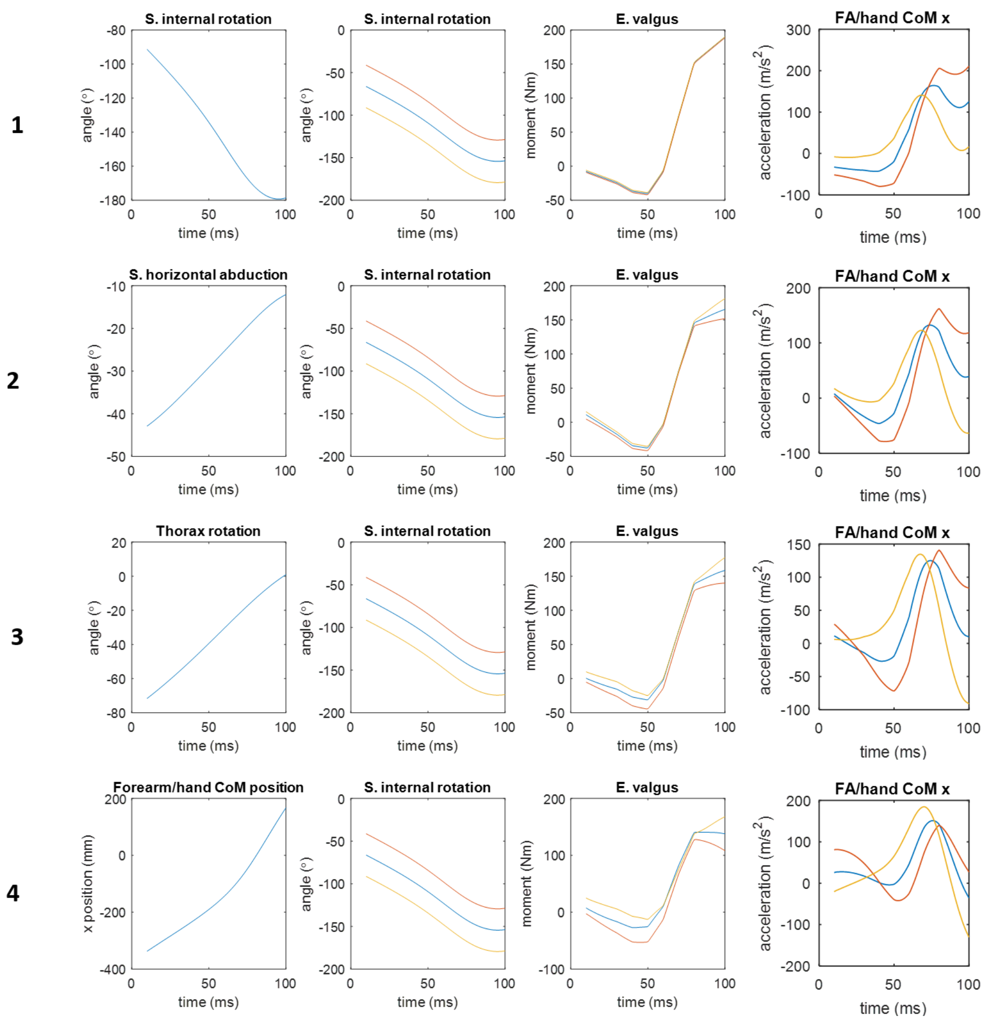

Figure 22: Influence of External Rotation (ER) variations.